

Experimental Determination of the Contribution of Chemical Sputtering of Carbon on Carbon Core Concentrations

M F Stamp, D Elder¹, H Y Guo, M von Hellermann,
L Horton, R König, J Lingertat, G McCracken, A Meigs,
P Stangeby¹, A Tabasso².

JET Joint Undertaking, Abingdon, Oxfordshire, OX14 3EA,

¹University of Toronto, Institute for Aerospace Studies, Ontario, Canada M3H 5T6.

²Imperial College, University of London, UK.

"This document is intended for publication in the open literature. It is made available on the understanding that it may not be further circulated and extracts may not be published prior to publication of the original, without the consent of the Publications Officer, JET Joint Undertaking, Abingdon, Oxon, OX14 3EA, UK".

"Enquiries about Copyright and reproduction should be addressed to the Publications Officer, JET Joint Undertaking, Abingdon, Oxon, OX14 3EA".

ABSTRACT

The effects of a methane puff at three different plasma locations has been compared with a similar deuterium puff in a 2.5MA, 2.5T Elmy H-Mode. Changes in edge and core spectroscopic signals have been examined, and show that divertor methane sources are much better screened than wall sources. An intrinsic outer divertor methane source is derived, and shown to account for only about 15% of the carbon in the plasma core. Modelling with EDGE2D/DIVIMP, using 0.5 eV carbon atoms for the methane source, has been performed and compared with the experimental results.

1. INTRODUCTION

The low Z and excellent thermal properties of carbon make it one of the best materials for the first wall (and divertor target) of a tokamak reactor. However, hydrogenic bombardment of carbon causes both physical and chemical sputtering. While physical sputtering can be minimised by having a very low edge electron temperature, chemical sputtering provides a source of methane (CD_4) and higher hydrocarbons which may enter and pollute the plasma.

It is difficult to accurately model the transport of methane because of the absence of good molecular rate coefficients for all the dissociation pathways of CD_4 and its break-up products. We have therefore performed a series of experiments to determine the effect of a known CD_4 source on the core carbon concentrations for the JET MkIIA divertor.

We have also used EDGE2D/DIVIMP to model these experiments in an attempt to judge the relative importance of the wall and divertor carbon sources, and their effectiveness in polluting the core plasma.

2. METHOD

The experiments were performed with a controlled CD_4 gas bleed into either (i) the private flux region (PFR), (ii) the outer scrape-of-layer (SOL) or (iii) the top of the vacuum vessel (TOP), in a 2.5MA, 2.5 Tesla, Elmy H-mode. Comparison discharges were then run with a D_2 gas bleed, with the same atomic deuterium source rate as the CD_4 pulse. Two types of target plasma were used, one with the strike points on the horizontal divertor tiles, and the other with the strike points on the vertical divertor tiles, fig.1. Gas fuelling from one of the divertor valves (see fig.1) therefore corresponds to SOL fuelling or PFR fuelling, depending on the

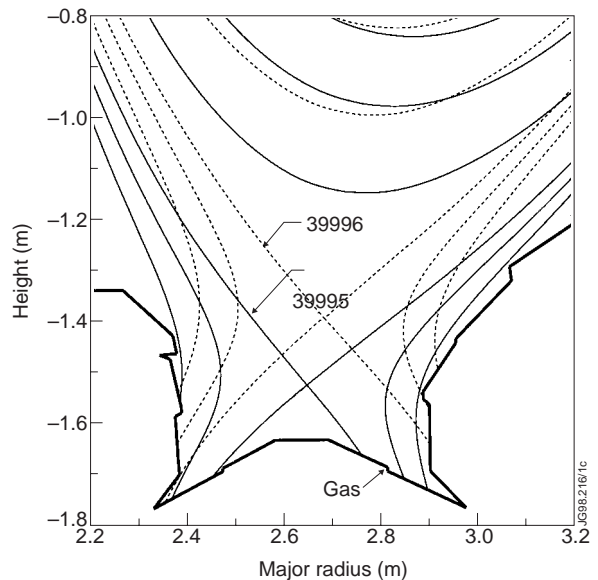


Fig. 1. X-point plasma configurations, showing the location of the divertor gas valve. SOL and TOP fuelling were performed with the horizontal target configuration (#39995), and PFR fuelling with the vertical target configuration (#39996).

strike point location. For TOP fuelling, a gas valve at the top of octant 6 was used with the horizontal target discharge. Note that TOP fuelling is at a single toroidal location, while fuelling into the divertor produces a toroidally symmetric gas input (via slits in pipes at 48 toroidal locations).

Passive visible, UV, VUV and X-ray diagnostics were used to monitor fuel and impurity line radiation and visible bremsstrahlung, and the active charge-exchange diagnostic was used to determine impurity density profiles.

3. EXPERIMENTAL RESULTS

The TOP, SOL and PFR fuelled discharge pairs were well matched, especially for the electron and ion temperatures, DD neutron rate, plasma stored energy and ELM behaviour, though the ELM's and ELM-free periods in the PFR fuelled (vertical target) discharges were irregular (fig.2). There were some small differences in the electron density (fig.3a) and NBI duration (fig.3b). The total radiated power (fig.4) was a little higher with CD₄ TOP fuelling and also showed the radiation spike from an inconel flake. Concomitant with this extra radiation, the ELM's changed from type I to type III.

We now look at the spectroscopic data, comparing typical between-ELM values, and

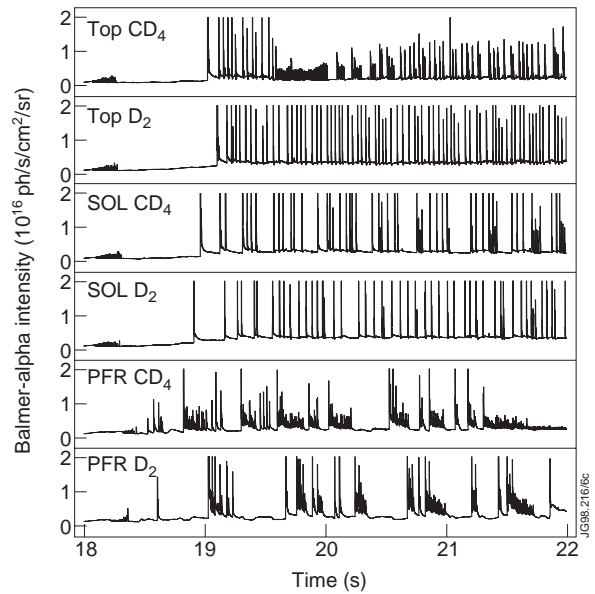


Fig. 2 Outer divertor Balmer-alpha intensity for the three pairs of shots, showing similar ELM behaviour in each pair.

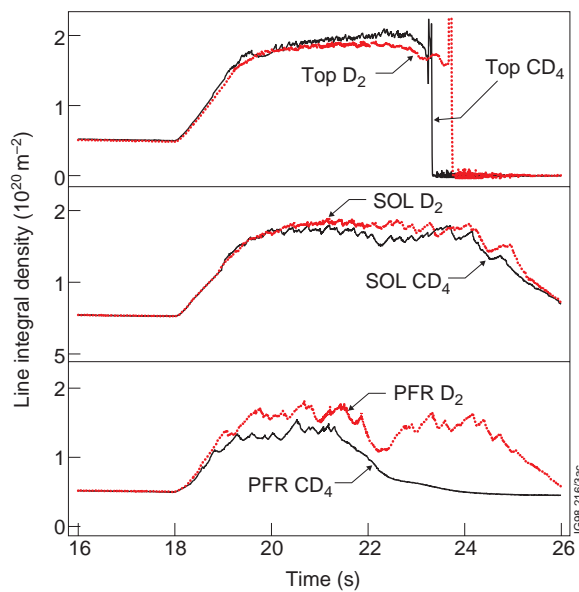


Fig. 3a. Survey of the line integral electron density for the three pairs of shots.

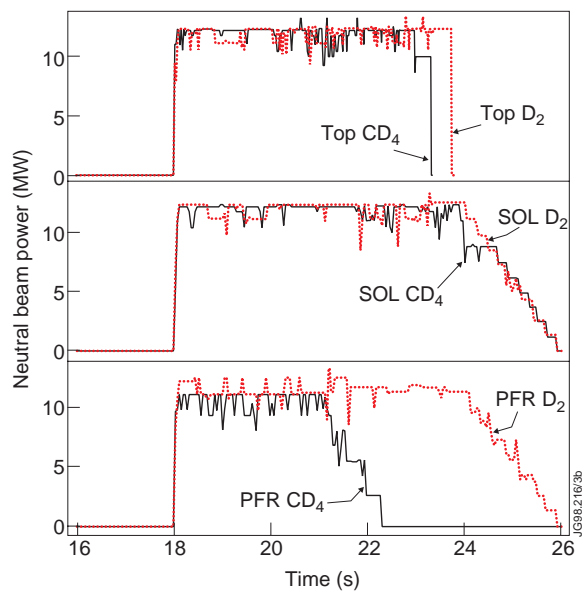


Fig. 3b. Survey of the Neutral Beam Injection Power for the three pairs of shots.

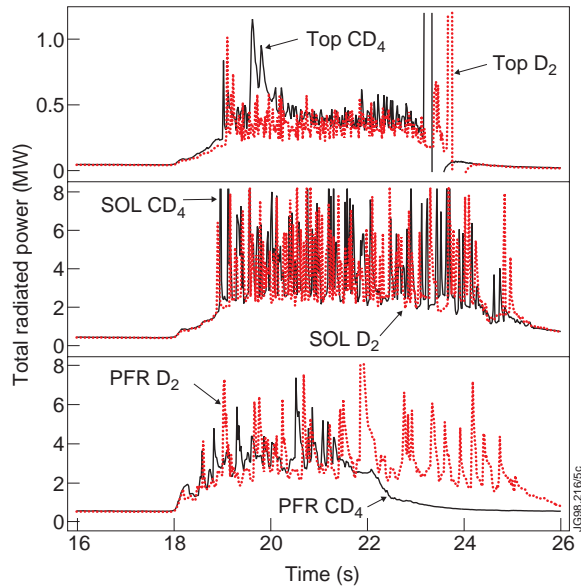


Fig. 4 Comparison of the total radiated power for the three pairs of shots.

start with the observations of the CD band intensity (431nm) at the inner and outer divertor, figs.5a,b. Clearly, TOP CD₄ fuelling did not change the inner or outer divertor CD signals, and outer divertor CD₄ fuelling into either the SOL or PFR had little or no effect on the inner divertor CD signal, whilst doubling the outer divertor CD signal. The C III (465nm) divertor signals behaved the same way, though the increase in signal with CD₄ fuelling was only about 30%. XUV measurements of C VI (3.37nm) on a horizontal line-of-sight showed no significant increases with either SOL or PFR CD₄ fuelling, though the signals were quite noisy. Visible wavelength measurements of C VI (529nm, n=7-8) (figs. 6a,b) showed no change at the inner divertor for both SOL and PFR CD₄ fuelling, and a small change at the outer divertor (less than about 10%).

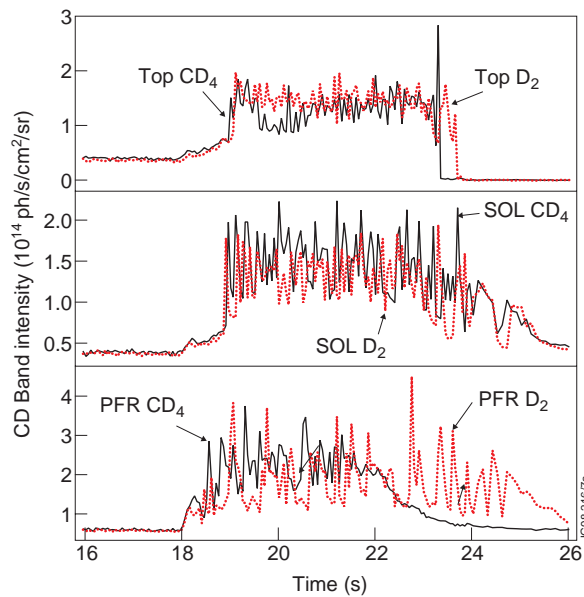


Fig. 5a. Comparison of the inner divertor CD band (431nm) intensities.

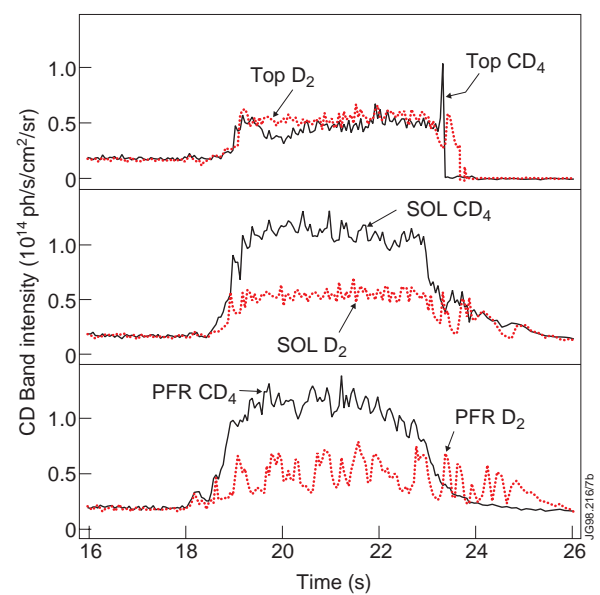


Fig. 5b Comparison of the outer divertor CD band (431nm) intensities.

The irregular nature of the ELM's in the PFR CD₄ and D₂ fuelled discharges makes a comparison of the inner divertor CD signals (fig.5a) somewhat subjective, but there does seem to be a higher signal level during ELM-free periods in the CD₄ fuelled discharge. The size of the difference is very approximately 3×10^{13} ph/s/cm²/sr (i.e. about half the outer divertor signal change), though the edge density and temperature were very different at the inner and outer strike points, so the photon efficiencies are probably different. We conclude that some of the

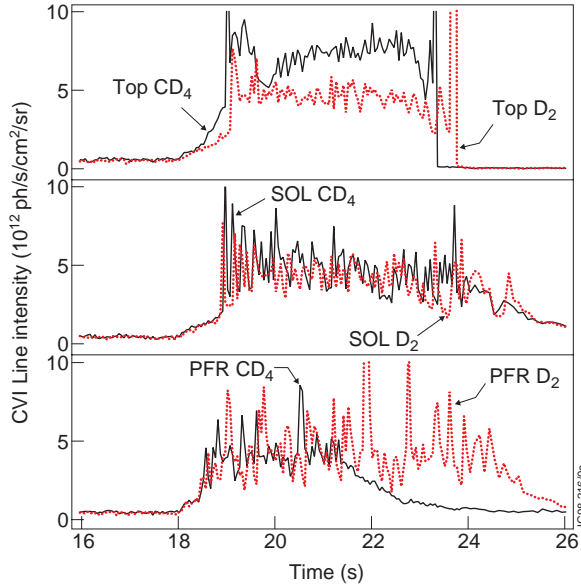


Fig. 6a Comparison of the inner divertor C VI line (529nm) intensities.

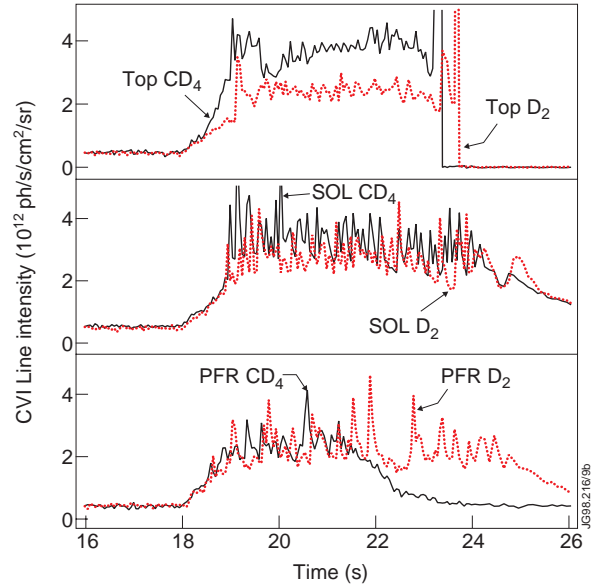


Fig. 6b Comparison of the outer divertor C VI line (529nm) intensities.

CD₄ puffed into the PFR near the outer strike point did manage to reach the inner divertor plasma.

TOP fuelling of CD₄ (at a single toroidal location) showed increased main chamber C II, C III, C IV and C VI signals (the CD signal was too weak to be observed), with the magnitude of the increase being largest on those lines-of-sight nearest the gas valve.

We turn now to indicators and measurements of the core carbon concentrations. It has been shown [1] that (radiated power / electron density squared) is proportional to $(Z_{\text{eff}} - 1)$. Figure 7 plots this parameter against time. SOL and PFR CD₄ fuelling showed a small increase (approximately 10%), but TOP fuelling showed the largest increase, about 40% if we compare before the perturbation from the inconel influx.

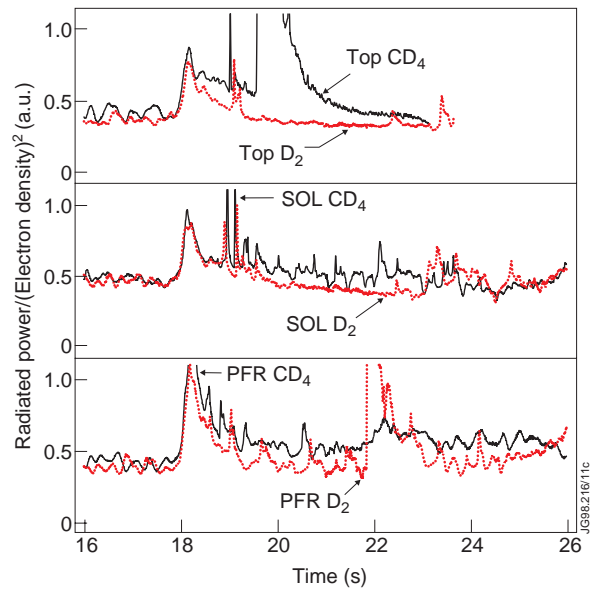


Fig. 7 Comparison of the bulk radiated power divided by the line integral electron density squared for the three pairs of shots.

The line-integrated Z_{eff} signal is shown in fig.8a, and contains noise contributions from the line-integrated visible bremsstrahlung (523nm) intensity and the LIDAR electron temperature and electron density profiles. A less noisy Z_{eff} signal is shown in fig.8b, where the bremsstrahlung intensity is divided by the line integral density squared. We can see that TOP CD₄ fuelling showed a 20% increase (and a clear increase caused by the inconel flake), while both SOL and PFR fuelling showed a 7% increase.

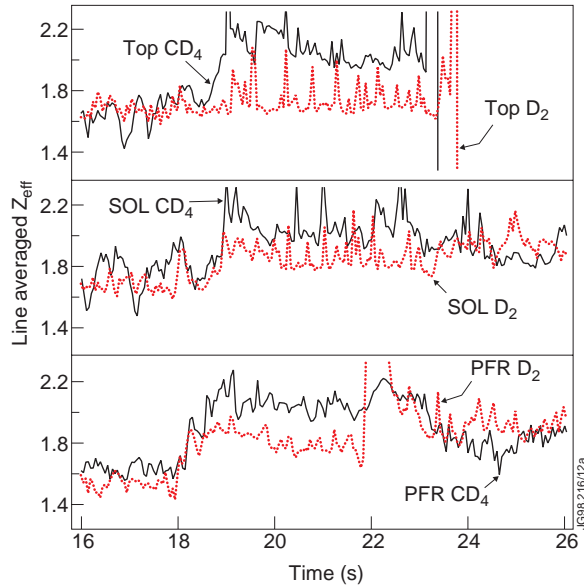


Fig. 8a Comparison of the line averaged Z_{eff} 's from a vertical line-of-sight.

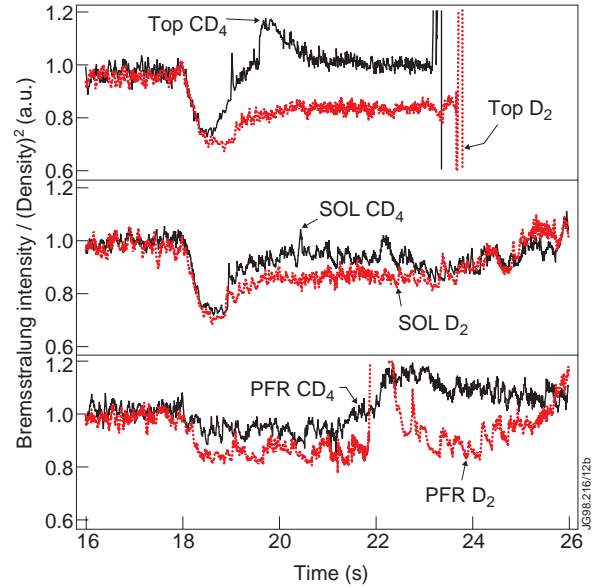


Fig. 8b Simplified Z_{eff} (bremsstrahlung divided by density squared). Note the increase in #39994 due to inconel flake!

Charge exchange measurements showed that the carbon density profile and the Z_{eff} profile were hollow, with similar shapes for CD_4 and D_2 fuelling. The uncertainties on the absolute carbon impurity density were rather high for these discharges, with the analysis giving a carbon density increase of about 40% for TOP CD_4 fuelling, and an increase of between 0-20% for SOL and PFR fuelling.

4. MODELLING

We have modelled the SOL D_2 fuelled discharge (#40000), using EDGE2D for the plasma background solution, and DIVIMP to follow the physical and chemically sputtered carbon impurities. The particle diffusion coefficient was taken to be $D_{\perp} = 0.1 \text{ m}^2/\text{s}$, with an inward pinch velocity, $V_{\text{pinch}} = 4.5 \text{ m/s}$, and $\chi_e = 0.2 \text{ m}^2/\text{s}$, $\chi_i = 0.4 \text{ m}^2/\text{s}$. ‘‘Toronto’97’’ chemical sputtering data [2] was used, with a yield reduction factor of 0.3 to allow for deuterium flux dependence and prompt redeposition of hydrocarbon fragments. The chemically sputtered carbon was launched by the codes as 0.5 eV carbon atoms.

The EDGE2D modelling required $P_e = 1 \text{ MW}$, $P_i = 3 \text{ MW}$ and $n_{\text{es}} = 1 \times 10^{19} \text{ m}^{-3}$ to match the J_{sat} and T_e profiles at the target plates. The divertor C II and Balmer-alpha emission profiles were also well matched, though the wall Balmer-alpha emission was underestimated by the code. This would suggest that the wall neutral pressure and the upstream separatrix density (n_{es}) were too low. Indeed, analysis by S Davies [3] on the relation between n_{es} and the volume average density using an ‘onion-skin’ model, indicates a value of $3.8 \times 10^{19} \text{ m}^{-3}$ for n_{es} for this discharge.

Figure 9 shows the EDGE2D/DIVIMP results for the carbon source and leakage (the amount of carbon that reaches the confined plasma) for different locations. We see that the chemically sputtered carbon source is everywhere larger than the physically sputtered source, and that the

total carbon source is largest at the outer and inner divertor. The leakage plot indicates that methane produced in the divertor is almost completely screened (about 10^{-3} screening efficiency for the outer divertor), while wall produced methane makes a significant contribution to core carbon (about 10^{-1} screening efficiency).

The model indicates that wall-produced carbon is contributing significantly to the core carbon, though it appears to be overestimating the screening efficiency for outer divertor (SOL) methane. From fig.9, doubling the outer divertor methane source would only result in a 2% increase in core carbon, whereas about a 15% change was seen experimentally.

The modelling was repeated with discrete methane puffs (TOP, SOL and PFR) added to the EDGE2D plasma solution. The above conclusions were confirmed, namely that the code gave essentially no leakage from SOL and PFR methane injection, while TOP injection gave more leakage than in the experiment. On the assumption that the gas injected was large enough to be causing parallel flows, such a parallel flow was then imposed in the code (running from the outer divertor round to the inner divertor). A parallel flow velocity of order 10^4 m/s was found to be sufficient to both (a) reduce the leakage for the TOP puff to about the experimental level, and (b) to increase the leakage for the SOL puff to about the experimental level (the imposed plasma flow away from the target is overcoming the frictional drag force). However, the methane and deuterium puffs could also be changing the local density and temperature, and this would also influence leakage.

5. CONCLUSIONS

Experimentally, 3×10^{21} molecules/s of TOP (i.e. wall) CD_4 fuelling does not have any effect on the low charge state divertor spectroscopic signals, but does increase the core carbon density by 40%.

The same CD_4 source injected into either the SOL or PFR doubles the outer divertor CD signal, increases C III by 30%, and increases core carbon by about 15%. Therefore the intrinsic outer divertor methane source must also be 3×10^{21} molecules/s, and this must contribute 15% to

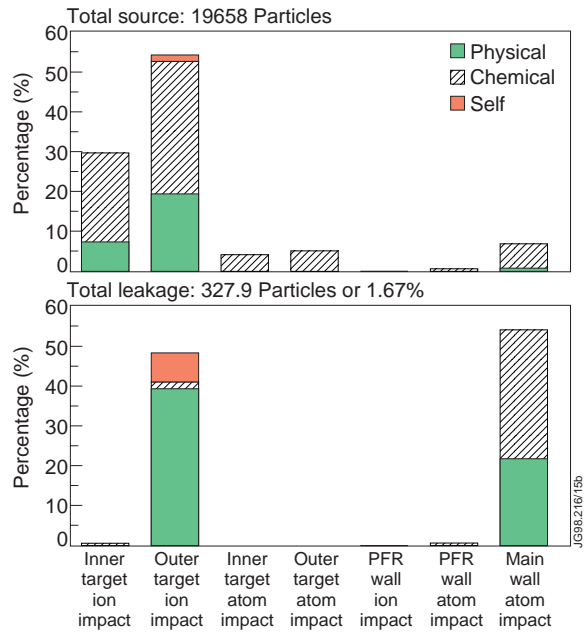


Fig. 9 EDGE2D/DIVIMP carbon source and leakage summary. The top section shows the percentage of the total source of 19658 particles that comes from the inner target, the outer target or the main wall via ion or atom impact. The lower section shows the same location information for the 328 particles that crossed the separatrix into the confined plasma.

the core carbon density in these steady-state Elmy H-modes. This is in contrast with Hot-Ion H-mode plasmas [4], where a much larger value is derived.

3×10^{21} molecules/s of CD_4 injected into the SOL increased the outer divertor CD band intensity by 5×10^{13} photons/s/cm²/sr. This implies a photon efficiency of 65 methane ionisations per CD photon, consistent with Behringer [5].

The similarity of the SOL and PFR fuelling results suggests that PFR methane source does not noticeably spread up to the X-point and contaminate the main plasma from there.

EDGE2D/DIVIMP modelling seems to overestimate the screening efficiency of the outer divertor for a methane source, and underestimate the screening for a wall methane source. If an additional parallel flow of order 10^4 m/s is imposed, then the modelling gives screening efficiencies consistent with experiment.

The EDGE2D/DIVIMP modelling indicates that in these steady-state Elmy H-modes, wall sources of carbon are as important as divertor sources in determining the core carbon density.

6. REFERENCES

- [1] G F Matthews, S Allen, N Asakura et al., J. Nucl. Mat. **241-243** (1997) 450.
- [2] B V Mech, A A Haasz and J W Davies, J. Nucl. Mat. **241-243** (1997) 1147.
- [3] S J Davies et al., these proceedings.
- [4] H Y Guo et al., these proceedings.
- [5] K Behringer, J. Nucl. Mat **176-177** (1990) 606.